

Article

A Mathematical Kinetic Model and Network Analysis for Multicomponent Dissolution Relationships during the Extraction of Natural Products

Yu Tang ^{1,2,3}, Yiqun Zhou ^{1,2,3}, Yutian Zhang ², Kaiwen Deng ⁴, Zhigang Liu ⁵, Wenlong Liu ^{1,2,3,*} and Fuyuan He ^{1,2,3,*}

- ¹ School of Pharmaceutics, Pharmacy College, Hunan University of Chinese Medicine, Changsha 410208, China; tangyuzi5655159@163.com (Y.T.); zhouyiqun0101@163.com (Y.Z.)
- ² Hunan Key Laboratory of Druggability and Preparation Modification for Traditional Chinese Medicine, Changsha 410208, China; rainyzyt@163.com
- ³ Supramolecular Mechanism and Mathematic-Physics Characterization for Chinese Materia Medicine, Changsha 410208, China
- ⁴ The First Affiliated Hospital of Hunan University of Traditional Chinese Medicine, Changsha 410007, China; pharmsharking@tom.com
- ⁵ No. 1 Traditional Chinese Medicine Hospital in Changde, Changde 415000, China; pharmqcpd@163.com
- * Correspondence: dragon5240@126.com (W.L.); 002172@hnuucm.edu.cn (F.H.); Tel.: +86-13974821547 (W.L.); +86-13787213681 (F.H.)

Abstract: Traditional Chinese Medicine (TCM) has a long history and typical ethnic traits. Astragalus and Angelica are used in a natural product called a buyang huanwu decoction and are considered to function as both food and medicine; such products are called a “homology of medicine and food”. In this study, we examined the complex extraction kinetics that occur during the preparation of the natural product BYHWD. Mathematical tools, including the Laplace transformation and Fick’s law, were used to set up kinetic equations for different components in a model of the decoction. We selected the five most important bioactive ingredients of the BYHWD to find the most important speed control component. The intensity and capacity process parameters of the model were determined. A kinetic model was used to quantitatively analyze the dissolution restriction mechanism among the major components. Further, a component–effect network relationship was established to study the interactions of different components during extraction, considering the integrative effect of TCM compositions. Finally, using network pharmacology, certain network parameters were determined through topological analysis. The results indicate that Astragaloside IV exerts the strongest control over the dissolution rates of other components. The BYHWD has a short average path and a high clustering coefficient. The theoretical and experimental results can be used to quantitatively simulate and optimize TCM extraction processes.

Keywords: natural product; buyang huanwu decoction; extraction kinetics; mathematical kinetic model; network kinetics; Traditional Chinese Medicine



Citation: Tang, Y.; Zhou, Y.; Zhang, Y.; Deng, K.; Liu, Z.; Liu, W.; He, F. A Mathematical Kinetic Model and Network Analysis for Multicomponent Dissolution Relationships during the Extraction of Natural Products. *Processes* **2022**, *10*, 1470. <https://doi.org/10.3390/pr10081470>

Academic Editors: Bonglee Kim and Carla Silva

Received: 16 June 2022

Accepted: 21 July 2022

Published: 27 July 2022

Publisher’s Note: MDPI stays neutral with regard to jurisdictional claims in published maps and institutional affiliations.



Copyright: © 2022 by the authors. Licensee MDPI, Basel, Switzerland. This article is an open access article distributed under the terms and conditions of the Creative Commons Attribution (CC BY) license (<https://creativecommons.org/licenses/by/4.0/>).

1. Introduction

The research on the extraction technology used for Chinese medicinal materials is an important and basic part of the research on the preparation technology used for Chinese medicinal materials. At present, orthogonal and uniform experimental design is mostly used to determine the optimal technological parameters of a single prescription under experimental conditions; however, this approach cannot clarify the relationship between the technological parameters of the extraction process used for the ingredients of medicinal materials [1]. Chinese medicinal materials have a cell membrane structure that is not conducive to the dissolution of the components in general solid preparations. As a result, the diffusion and dissolution of components are greatly hindered. At the same time,

Chinese medicinal materials are often irregularly shaped yinbian, which can absorb several times more solvent and expand. High-temperature extraction of medicinal materials leads to ease of decomposition. On the basis of previous studies, this study established, for the first time, mathematical parameters related to extraction kinetics and established a three-compartment mathematical model that laid a theoretical foundation for quantitative research and the further optimization of the extraction processes of TCM.

The buyang huanwu decoction (BYHWD) is a TCM formulation, and it has six ingredients: astragalus, Angelica, peony root, peach kernel, safflower, and earthworm [2,3]. Astragalus and Angelica are widely used and are edible TCM herbs. They are rich in saponins, flavonoids, phenolic acids, amino acids, vitamins, and multiple other essential bioactive ingredients. This article focuses on the homology of medicine and food used in the BYHWD and emphasizes the bioactive ingredients and their extraction kinetics and network kinetic effects. In this study, solid differential equations were set up to model the extraction process and calculate all kinetic parameters. The kinetic model was based on diffusion law and took into account solid expansion, solid-to-liquid mass transfer, and the Noyes–Whitney dissolution theory for the solid components. These differential equations were used to quantitatively predict the dissolution and diffusion of TCM components and optimize the extraction process. Furthermore, the most important dissolution rates were obtained. This model is the first application of these theoretical tools to the TCM extraction process, and it can provide a quantitative assessment of the process parameters and allow the numerical simulation of the dissolution process. The results are expected to advance the study of the dissolution kinetics of TCMs [4,5].

Model Assumptions

Dried herbal pieces swell after soaking in solvents before active ingredients are extracted [6]. The plant cell walls and membranes act as barriers to component dissolution and diffusion [7,8]. Therefore, these structures need to be explicitly taken into account in related mathematical modeling [9]. Following dissolution, diffusion occurs throughout the cell protoplasm (i.e., the material within the cell cytomembrane, which is referred to herein as the ‘compartment in cell’ (CIC)). Thereafter, the dissolved components move into the apoplasm (a contiguous area between the cell membrane and the cell wall), which acts as an extracellular capillary expansion chamber, and finally into the solution chamber (i.e., the compartment in solution (CIS)) through the cell wall.

The component extraction process is illustrated in Figures 1 and 2. G_0 , S_0 , and I_0 denote the solid TCM, solvent, and active ingredients, respectively. The total amount of I_0 is W . Initially, the concentration of I_0 in the CIC (effective volume: V_0 ; effective surface area: A_1) is C_0 . The dissolved components diffuse outside the cell membrane into the apoplasm, which has an effective volume of V_1 , an effective surface area of A_2 , and a concentration of C_1 for component I_0 . Finally, I_0 diffuses into the solution chamber, where it has a concentration of C_2 in a volume of V_2 . As the ratio of soluble components, i.e., I_0 , to the solvent is relatively low, I_0 can be considered to initially dissolve completely in the CIC at a high C_0 . Then, the active components diffuse from the protoplasm into the apoplasm with the mass transfer coefficient k_1 . The concentration ratio (or partition coefficient, i.e., C_0/C_1) of I_0 between these two chambers is ρ_1 . Next, I_0 further diffuses into the solvent chamber S_0 with the mass transfer coefficient k_2 , where $\rho_2 = C_1/C_2$. Meanwhile, the component may also be eliminated from the solution chamber owing to decomposition, with the rate constant k . Using Fick’s law [10], the Noyes–Whitney dissolution theory (where C and C_s represent the actual concentration at time t and the solubility, respectively, and k is the dissolution rate constant), the dynamic principle, and the Laplace transformation, a system of differential equations can be constructed and solved under the initial conditions $C_{1,0} = 0$ and $C_{2,0} = 0$ for $t = 0$ to obtain C_2 at different times (i.e., the composition of the extract) [11].

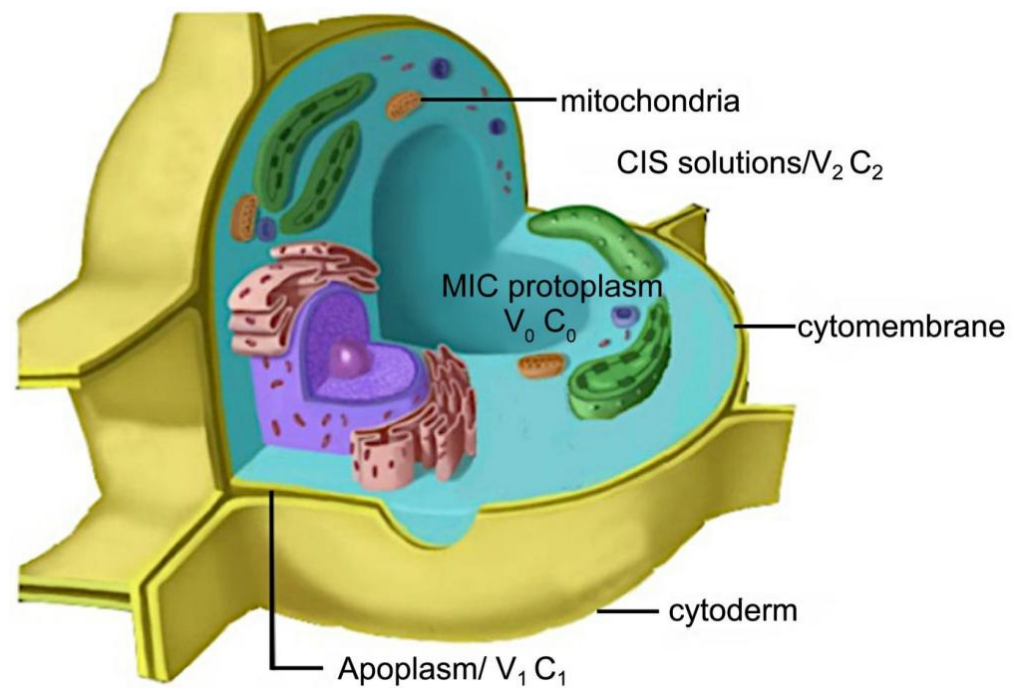


Figure 1. Illustration of the different chambers in composition dissolution.

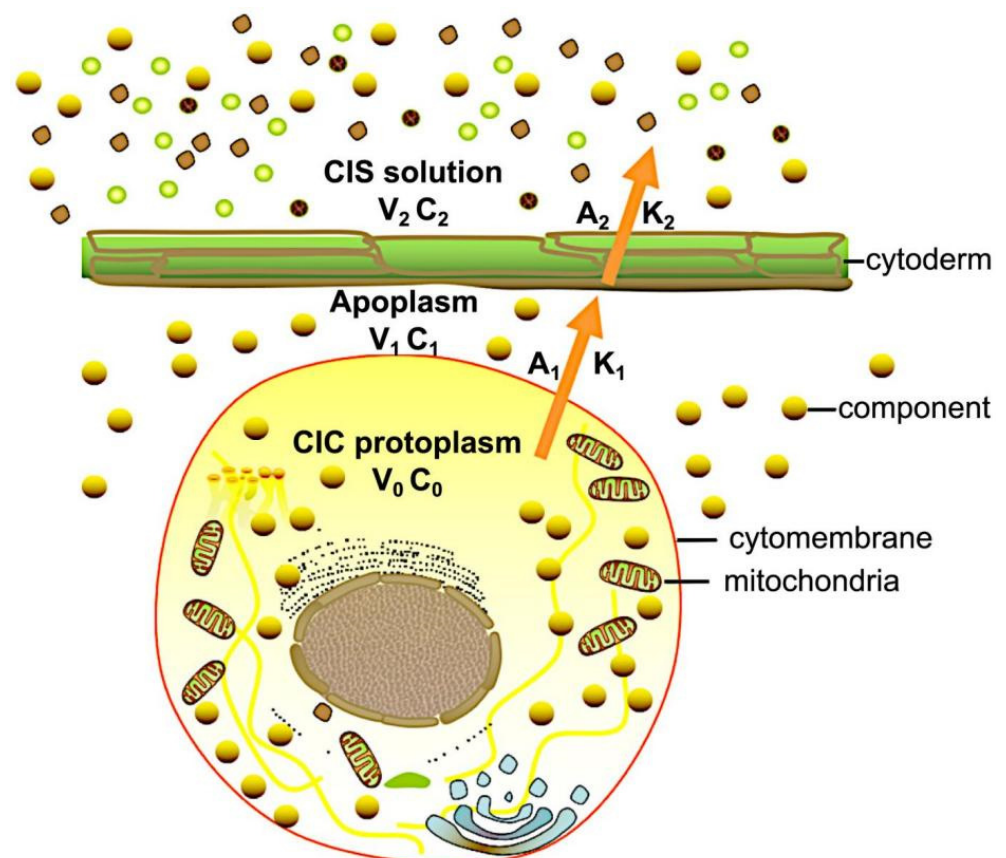


Figure 2. Cross-sectional view of composition dissolution in the cells.

To study the kinetics of the BYHWD [12], it is necessary to also consider the relationships among its important components. The complex sets of chemicals in TCMs can be regarded as nodes. These components dissolve and diffuse in the solvent, and their interactions during this process can then be modeled as a network. The resultant network

can be described by a few parameters, such as the degree, density, average degree, average path length, network diameter, and clustering coefficient of the network.

Herbal component tissues are usually subjected to certain pretreatments before drying in order to minimize the occurrence of adverse changes during drying and subsequent storage. Rehydration is the process of moistening dry material. The rehydration process itself may also affect the tissue.

Mostly, rehydration is performed by the addition of an abundant amount of water. Dry material submerged in water undergoes many changes that are the result of water imbibition and solute loss. When dried herbal pieces swell after soaking in a solvent to extract the active ingredients, it is considered a rehydration process. Water absorption by dry material consists of various processes with different kinetics. During rehydration, a substantial amount of soluble materials leach into the surrounding water. Diffusion is a prevailing mechanism, and Fick's second law should provide a good fit to the experimental data. The moisture uptake of herbal material is closely related to factors that include surface area, capillary suction, porosity, concentration of surface moisture, temperature, and others. These factors should also be taken into consideration in future experiments [13].

2. Materials and Methods

2.1. Materials and Instruments

The dried herbs to prepare the BYHWD were manufactured by the Pharmacy Department of the Hunan University of Traditional Chinese Medicine (Changsha, China). Detection was carried out using high-performance liquid chromatography (HPLC; Waters Breeze, Dual Absorbance Detector, 2487 Workstation) (Milford, MA, USA). HPLC-grade acetonitrile and methanol were purchased from Shanghai SSS Reagent Co., Ltd. (Shanghai, China), and other reagents were of pure grade (i.e., 99.7% pure). The water was redistilled, and 1% aqueous acetic acid solution was used as the mobile phase. Five standards were purchased from Changsha Pharmaceutical Laboratory (Changsha, China): Astragaloside IV (AST-IV, 110781-201213), paeoniflorin (PF, 110736-201451), Laetrile (LT, 110736-201412), ferulic acid (FA, 110736-201337), and ligustrazine (LS, 110736-201324). All samples, drugs, and reagents were weighed using the Metler Toledo AG 214 balance (Zurich, Switzerland).

2.2. Mathematical Basis of the Extraction Model

For each of the five studied components ($I_0 = \text{AST-IV, PF, LT, FA, and LS}$), the value of W_0 was determined at a given temperature. If the sample piece/particle sizes were known, A_1 and A_2 could be determined. In the extraction chamber, k , k_1' , and k_2' could be determined, and the component I_0 was dissolved according to C_2 dissolution kinetics. The process parameters (i.e., W_0 , A_1 , A_2 , V_0 , V_1 , V_2 , ρ_1 , ρ_2 , k , k_1' , and k_2') and the parameters that measured the extraction effect (t_{\max} , $C_2 \max$, P , and D) were measured. According to Fick's law, Noyes–Whitney's stripping theory, and the actual situation of the extraction process, a mathematical model of the stripping kinetics of the TCM compound was established, including algebraic calculus equations, and the function expression was obtained [14–16].

2.3. Solving Extraction Equations in the Model

Using the experimental data, the parameters α , β , π , M , N , and L were estimated using the multivariate curve residual method or the statistical package for the social sciences (SPSS) (version 16) (Beijing, China) according to the relevant calculation formula to obtain K , ρ_1 , k_1' , and k_2' [2].

2.4. Statistical Moment Analysis of the Kinetic Network

In the field of kinetics, the first moment is the mean residence time (MRT) of a drug, and the second moment is the variance of residence time (VRT), which indicates the time span of a drug's metabolism [17]. Based on the calculated MRT and VRT values, the composition with the most additive component is likely the main regulator of the extraction rate. However, the content of the components should also be considered.

MRT and VRT were calculated from the area under curve (AUC) data. The zeroth moment is the sum of all components, as shown in Equation (1).

$$AUC_t = AUC_i = \sum_{i=1}^m \sum_{j=1}^{r_i} \frac{M_{i,j}}{\alpha_{i,j}} + \sum_{l=1}^{s_1} \frac{2k_{m,l}c_{0,l} + c_{0,l}^2}{2V_{m,l}} + \sum_{q=1}^{s_2} \int_0^{\infty} C_{nr}, q^{dt} \quad (1)$$

where m is the number of linear components, r_i is the number of chambers for component i , and s_i is the number of nonlinear components. MRT, being the population mean of the components, is defined as follows:

$$MRT = \frac{\sum_{i=1}^n MRT_i \times AUC_i}{\sum_{i=1}^n AUC_i} \quad (2)$$

Similarly, the second moment, VRT, is written as:

$$VRT = \frac{\sum_{i=1}^n [(MRT_i^2 + VRT_i)] \times AUC_i}{\sum_{i=1}^n AUC_i} - MRT^2 \quad (3)$$

The relationship between the concentration of components and the extraction time was shown in Equation (4)

$$\begin{aligned} C_2 &= \frac{k_1'k_2'w_0}{V_0(\beta-\alpha)(\pi-\alpha)}e^{-\alpha t} + \frac{k_1'k_2'w_0}{V_0(\alpha-\beta)(\pi-\beta)}e^{-\beta t} + \frac{k_1'k_2'w_0}{V_0(\alpha-\pi)(\beta-\pi)}e^{-\pi t} \\ &= \frac{k_1'k_2'c_0^0}{(\beta-\alpha)(\pi-\alpha)}e^{-\alpha t} + \frac{k_1'k_2'c_0^0}{(\alpha-\beta)(\pi-\beta)}e^{-\beta t} + \frac{k_1'k_2'c_0^0}{(\alpha-\pi)(\beta-\pi)}e^{-\pi t} \\ &= Me^{-\alpha t} + Ne^{-\beta t} + Le^{-\pi t} \end{aligned} \quad (4)$$

2.5. Theoretical Formulation of Network Analysis for the Extraction Model

A method for calculating the network pharmacology combined with the principle of chemical kinetics has been previously reported [2]. All nodes and their interactions form a topological network [18]. The kinetic relationship of the nodes can be expressed by the corresponding kinetic Equation (5).

$$A(a_{ij}) = K(k_{ij}) \quad (5)$$

The basic assumption is that an increase or decrease in the flow at each node affects the algebraic sum of the two nodes with positive action (+) and negative action (-). The general diagram is shown in Figure 3.

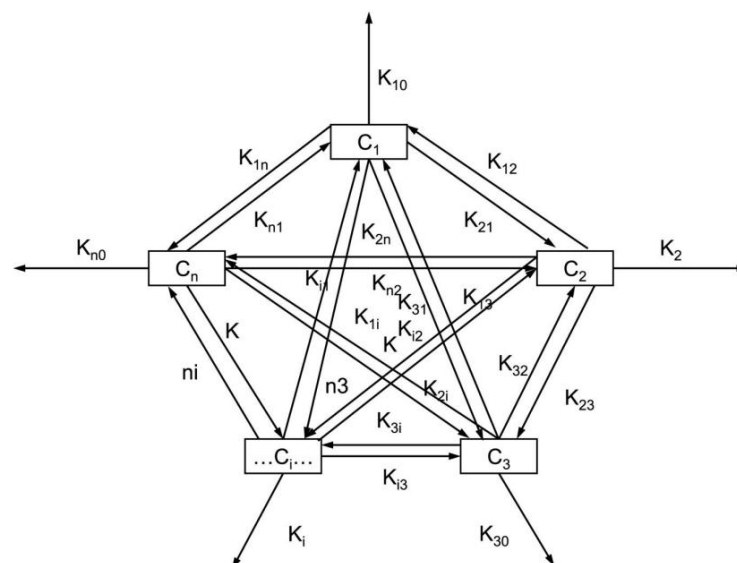


Figure 3. Representative model of n-node network dynamics.

2.6. Concepts of Other Parameter Network Dynamics

The network density (D) refers to the percentage of existing connections among all possible connections. The out-degree is the number of edges linking one specific node to other nodes in the network. In TCM network analysis, the out-degree represents the simultaneous effect of one component on other components. The in-degree is the number of edges linking other nodes to a specific node, and it represents the degree of effectors on that node. The sum of the out-degree and in-degree for a node is the node degree, which represents the extent to which one component is constrained by other components. The average node degree is the sum of edges divided by the number of nodes. The network diameter is the maximum value of the shortest path between each node and another node. The ratio of the number of connections to/from a node vs. the maximum possible number of connections is the clustering coefficient.

2.7. Sample Preparation

2.7.1. Collection of Samples at Different Times

A sample of the dried herbal mix (111 g) was weighed precisely and mixed with 888 mL of distilled water (1/8 w/w) in a three-necked round-bottom flask. One neck was connected to a condenser, another connected to a quantitative sampler, and the third connected to a thermometer. The whole device was kept in a water bath. Time 0 was defined as when the reflux temperature was achieved and the first drop of condensed water fell off. Samples for HPLC measurement were collected in 2 mL aliquots at 5, 10, 20, 30, 60, 90, 120, 180, 240, 360, 720, 1335, and 1440 min.

2.7.2. Determination of Protoplasm, Apoplasm, and Solution Volumes

A dried herbal sample of weight W_1 was placed in a 500 mL flask. Thereafter, distilled water at 100 °C was added to the mark, and the weight was recorded as W_2 . The flask was kept at 100 °C for 2 h to allow the pieces to fully swell. The entire volume of liquid was then poured into a 500 mL graduated cylinder to measure $V_{\text{discharge}}$. Here, $V_2 = 500 - V_{\text{discharge}}$, and $V_1 + V_0 = (W_2 - W_1)/d_{\text{water}} - V_2$; d_{water} is the specific gravity of water. The apoplasm volume (V_1) was then determined by centrifugation of the swollen herbs. The supernatant volume was measured and plotted against the centrifugal rate (1000–5000 rpm), and the saturation volume was determined as V_1 . Finally, V_0 was determined based on the ($V_1 + V_0$) value described above. Hence, V_0 , V_1 , and V_2 were all obtained.

2.7.3. Determination of the Distribution Coefficients ρ_1 and ρ_2

The concentrations of the five main components in the decoction (AST-IV, PF, LT, FA, and LS) were measured for liquids in the solution chamber and apoplasm chamber, using the differential anthrone–sugar hydrazone method. Please see ref. [19] and HPLC fingerprints (described below). These results allowed the calculation of ρ_2 .

2.7.4. HPLC Quantitative Analysis

For the HPLC determination conditions, refer to the State Pharmacopoeia. The HPLC analysis used an Ultimate XB-C18 column (250 mm × 4.6 mm, 5 μm), and the flow phases were 1% acetic acid (aq.) and acetonitrile. The gradient elution was as follows: 0 min (water:acetonitrile = 100:0) → 10 min (100:0) → 25 min (93:7) → 5 min (87.5:12.5) → 5 min (82:18) → 65 min (75:25) → 65 min (70:30) → 70 min (67.5:32.5) → 71 min (67:37) → 80 min (60:40) → 100 min (20:80) → 115 min (0:100) → 120 min (100:0) → 123 min (100:0). The flow velocity was 1.0 mL·min⁻¹, the UV detector monitored the wavelength of 264 nm, the temperature was 40 °C, and the injection volume was 20 μL . The linearity, accuracy, precision, stability, recovery, and specificity were assessed [20].

The HPLC–ELSD determination of AST-IV was as follows: the flow phase was methanol:water (75:25), and the flow rate was 0.8 mL·min⁻¹. The column temperature was 30 °C, and the drift tube temperature was 100 °C. The nitrogen flow rate was 2.5 mL·min⁻¹.

The injection volume was 20 μL . The theoretical plate number should be no less than 4000 according to the peak of AST-IV.

The linearity, accuracy, precision, stability, recovery, and specificity were assessed [21].

2.7.5. Preparation of Reference Solution

The paeoniflorin (2.4 mg), Astragaloside iv (4.0 mg), amygdalin (2.6 mg), ferulic acid (1.8 mg), and ligustrazine (2.0 mg) were carefully weighed and placed in a 5 mL volumetric flask, dissolved in chromatographic pure methanol, and then filtered by a 0.45 μm microporous membrane. A mixed standard solution containing PF 0.48 $\text{mg}\cdot\text{mL}^{-1}$, AST-IV 0.8 $\text{mg}\cdot\text{mL}^{-1}$, LT 0.52 $\text{mg}\cdot\text{mL}^{-1}$, FA 0.36 $\text{mg}\cdot\text{mL}^{-1}$, and LS 0.4 $\text{mg}\cdot\text{mL}^{-1}$ was prepared.

2.7.6. Preparation of Sample Solution

The entire quantity of the BYHWD formula was transferred into a 500 mL round-bottom flask, eight times the amount of water was added, and it was placed on the electric stove for heating before being boiled for half an hour; then, the liquid was cooled, and the extract was dried. A quantity of 0.02 g of dry matter was accurately weighed in a 10 mL volumetric flask, and methanol was added to dissolve at constant volume; then, it was filtered through a 0.45 μm microporous membrane to prepare the sample solution, which was set aside.

3. Results

3.1. HPLC Fingerprints of the BYHWD

We obtained the HPLC fingerprints of the BYHWD. 13 HPLC fingerprints of BYHWD sample solution that collected at 5, 10, 20, 30, 60, 90, 120, 180, 240, 360, 720, 1335, and 1440 min. have shown in Figure 4. A chromatogram of AST-IV, LS, LT, PF, and FA analytical standards have shown in Figures 5 and 6.

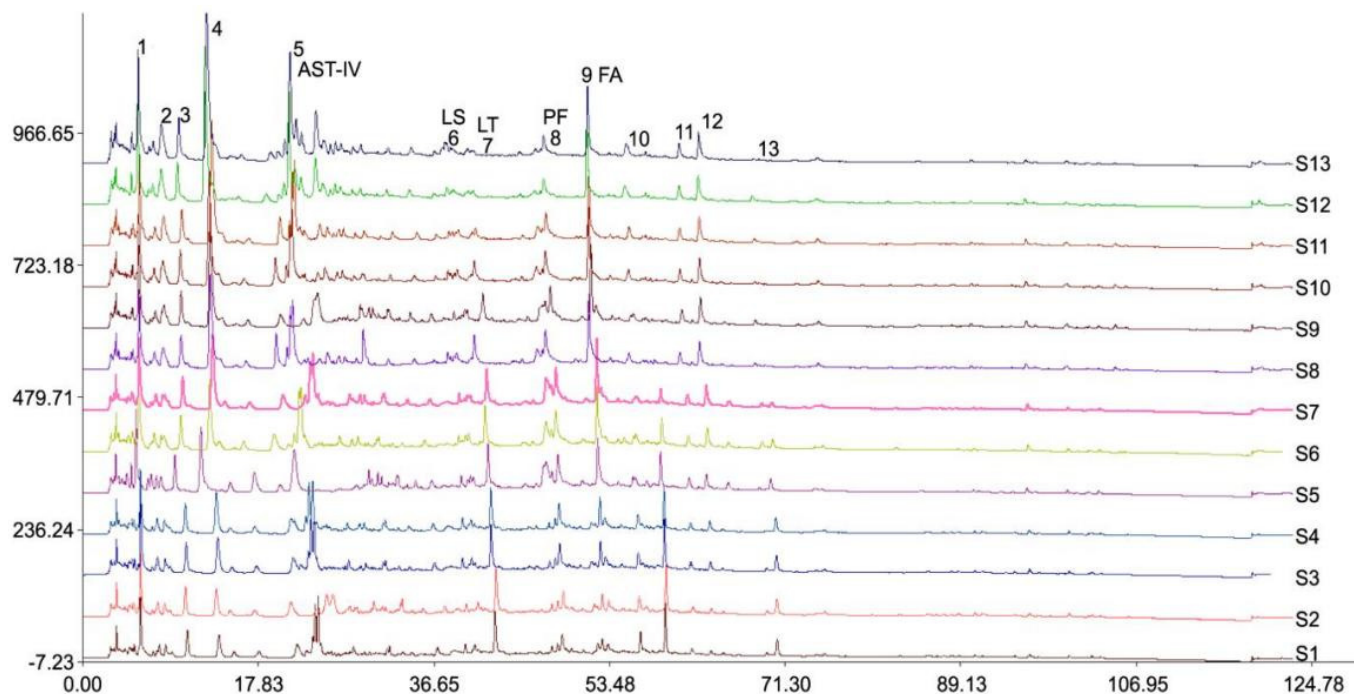


Figure 4. HPLC fingerprints of the BYHWD extracts sampled at different time points. S1-S13:13 HPLC fingerprints of BYHWD sample solution were collected at 5, 10, 20, 30, 60, 90, 120, 180, 240, 360, 720, 1335, and 1440 min.

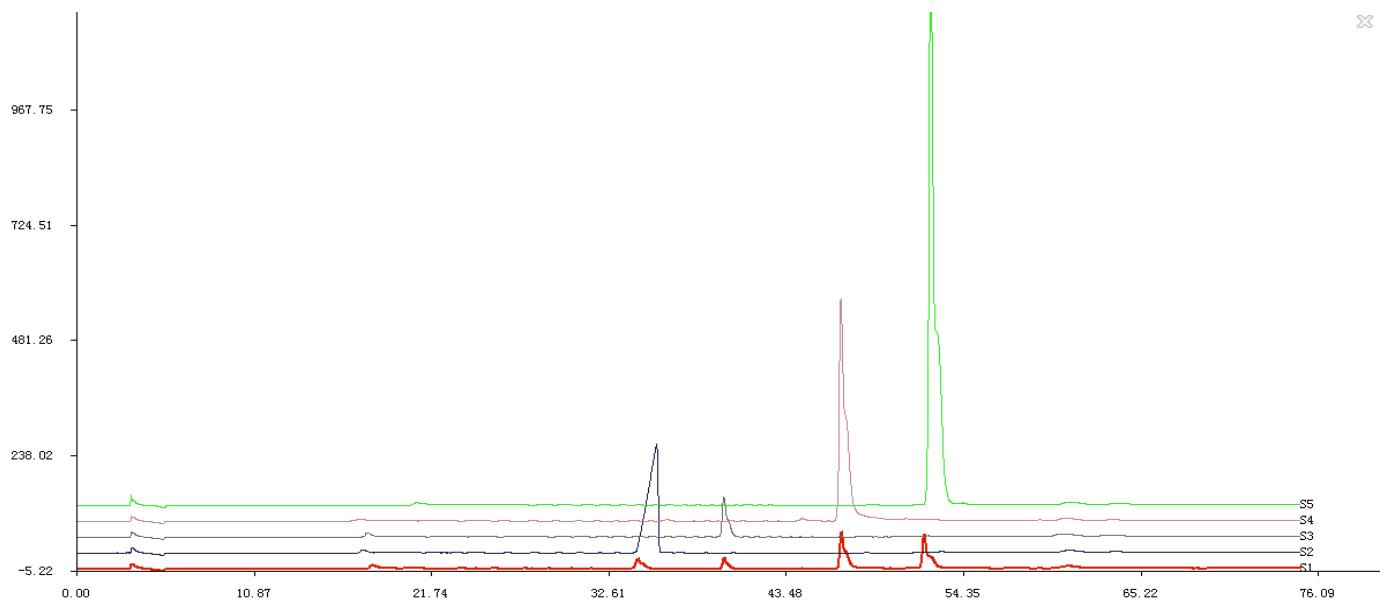


Figure 5. HPLC peaks of four standard products of the BYHWD. S1. Mixture of reference substance; S2. LS standard; S3. LT standard; S4. PF standard; S5. FA standard.

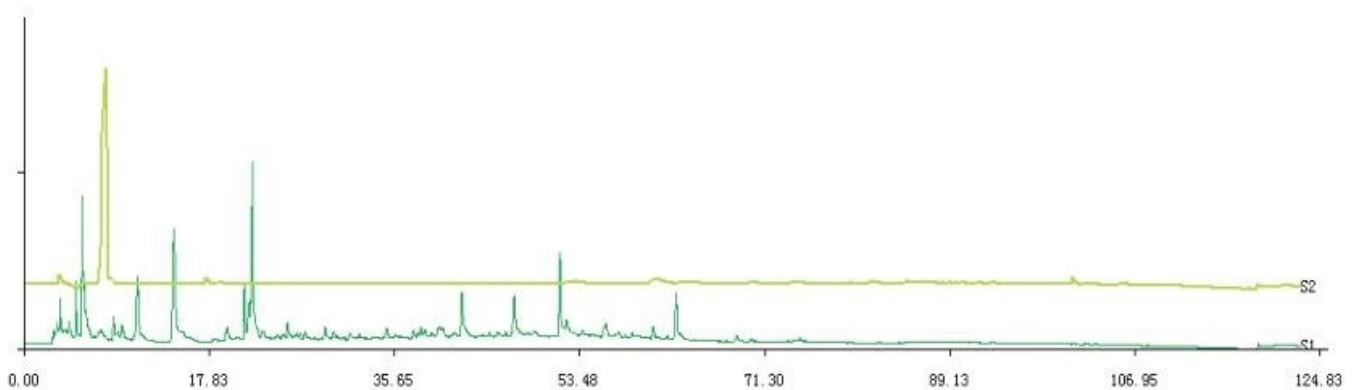


Figure 6. HPLC-ELSD peaks of AST-IV. S1. Sample solution of the BYHWD; S2. AST-IV standard.

3.2. HPLC Quantitative Analysis

3.2.1. Linearity Test

Quantities of 10, 5, 1, 0.5, and 0.1 mL of the reference solution were accurately absorbed and diluted to 10 mL with methanol at constant volume; then, 20 μL was injected through a 0.45 μm microporous membrane. The peak area of the standard substance was used to determine the linear regression of the concentration, and the related linear regression equations were obtained: AST-IV $Y = 2.1 \times 106X - 1043$ ($R^2 = 0.9995$); PF $Y = 4.2 \times 106X - 94530$ ($R^2 = 0.9934$); LT $Y = 1.5 \times 106X - 34500$ ($R^2 = 0.9912$); FA $Y = 3.2 \times 107X - 84590$ ($R^2 = 0.9812$); and LS $Y = 5.4 \times 106X + 23510$ ($R^2 = 0.9943$). The linear ranges of the five standard samples were 1.24~59.4, 4.25.64~479.00, 1.14~182.0, 6.3~4.00, and 1.89~178.00 $\mu\text{g}\cdot\text{mL}^{-1}$.

3.2.2. Precision Test

The peak area RSDs of AST-IV and PF were 1.03% and 0.34%, respectively. LT was 0.35%; FA was 0.45%; LS was 0.96%.

3.2.3. Repeated Test

The peak area RSDs of AST-IV, PF, LT, FA, and LS were 0.34%, 0.26%, 0.31%, 0.12%, and 0.96%, respectively.

3.2.4. Stability Test

The peak area RSDs of AST-IV, PF, LT, FA, and LS were 0.65%, 0.63%, 0.35%, 0.45%, and 0.76%, respectively, at 0, 2, 4, 6, 8, and 24 h after sample solution preparation.

3.2.5. Recovery Test

Six samples of 100 μL each were taken, and control was added in quantities of 50, 100, 150, 200, 250, and 300 μL . The recovery of AST-IV was 98.1%, and its RSD was 1.04%. PF's recovery was 99.4%, and its RSD was 1.54%. LT's recovery was 100.1%, and its RSD was 2.21%. FA's recovery was 98.7%, and its RSD was 0.92%. LS's recovery was 96.7%, and its RSD was 1.35%.

3.3. V_0 , V_1 , and V_2 Values

When the liquid centrifuged from the apoplasm stopped increasing with increasing rotation speed, the volume of the solution in the apoplasm was determined to be 67.5 mL. Hence, we determined that $V_1 = 67.5$ mL, $V_0 = 104.6$ mL, and $V_2 = 218.5$ mL.

3.4. Concentrations of Total and Main Glycosides in Dried Herb Samples

The total concentration of glycosides as determined using the differential anthrone—sugar hydrazine colorimetry method was 75.30%, and the amounts of AST-IV, PF, LT, FA, and LS as determined by HPLC were 1.231%, 0.2563%, 0.3521%, 0.210%, and 0.467%, respectively.

3.5. Calculation of the Distribution Coefficients ρ_2 and ρ_1

Using the above data, the ρ_2 value for the total glycosides was determined to be 0.3210, whereas the values for AST-IV, PF, LT, FA, and LS were 1.069, 1.046, 1.154, 1.021, and 0.787, respectively. The results for the glycoside groups and main glycosides are listed in Table 1. Based on the results in Table 1, the extraction concentrations of the five components in the BYHWD from 0 to 1440 min are plotted in Figure 7.

Table 1. Contents of total glycosides and the five main components at different extraction times.

Extraction Time/min	Total Glycosides/ $\text{mg}\cdot\text{mL}^{-1}$	AST-IV/ $\mu\text{g}\cdot\text{mL}^{-1}$	PF/ $\mu\text{g}\cdot\text{mL}^{-1}$	LT/ $\mu\text{g}\cdot\text{mL}^{-1}$	FA/ $\mu\text{g}\cdot\text{mL}^{-1}$	LS/ $\mu\text{g}\cdot\text{mL}^{-1}$
5	24.39	36.1	17.12	48.43	5.21	4.45
10	28.28	38.1	18.54	49.65	6.45	6.38
20	33.53	42.54	19.76	50.54	6.65	7.09
30	35.49	54.76	20.65	51.76	9.87	8.66
60	38.22	67.43	21.66	50.68	16.94	12.98
90	40.94	76.54	23.53	50.11	23.08	14.07
120	48.98	80.65	24.54	50.98	28.39	15.24
180	46.45	85.43	25.87	49.01	36.56	16.09
240	41.65	86.54	26.43	47.11	42.55	17.11
360	35.21	98.21	29.43	42.54	52.8	18.59
720	33.09	93.65	31.19	35.44	63.99	19.14
1355	32.66	90.23	34.43	27.65	70.03	20.09
1440	17.70	89.22	36.65	26.95	70.5	21.17

AST-IV, Astragaloside IV; PF, paeoniflorin; LT, Laetrile; FA, ferulic acid; LS, ligustrazine.

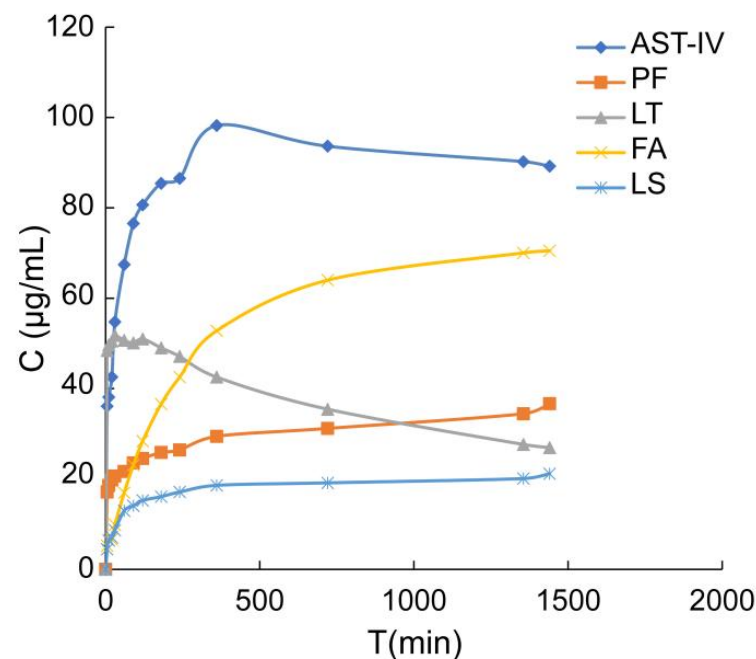


Figure 7. Time-dependent concentrations of the five main components.

3.6. Curve Fitting

Next, the initial values of M , α , N , β , L , and π were obtained using the residual method according to the three-compartment model. The regression equations and correlation coefficients were evaluated using SPSS to obtain the multivariate nonlinear parameters (the sampling frequency (N) and the correlation coefficient (R^2)).

Table 2 presents the results for the related kinetic parameters. The dissolution kinetics of the five main components conformed to the three-compartment model ($p < 0.01$). By substituting the results into the relevant equations, the kinetic parameters, including k_1' , k_2' , ρ_1 , t_{max} , c_{max} , P , D , and others, were determined (Table 3).

Table 2. Extraction kinetic curve fitting and the parameters of total glycosides and the five main components.

Parameter	Total Glycosides	AST-IV	PF	LT	FA	LS	Additive Component
$M/\%$	0.7016	0.1187	0.7269	0.2902	0.3063	0.4654	0.4930
α/min^{-1}	0.00406	0.00959	0.00201	0.00103	0.00305	0.00902	0.00874
$N/\%$	-0.6306	-0.2298	-0.6963	-0.1903	-0.1887	-0.4101	-0.4696
β/min^{-1}	0.02244	0.0225	0.0625	0.0284	0.01768	0.00707	0.01358
$L/\%$	0.09494	0.0219	0.04799	0.07816	0.01432	0.1446	0.09297
π/min^{-1}	0.001078	0.0088	0.07597	0.01154	0.04416	0.0141	0.9.615
R	0.846	0.977	0.984	0.940	0.943	0.9860	0.996
N	34	45	109	24	13	24	23
p	<0.01	<0.01	<0.01	<0.01	<0.01	<0.01	<0.01

The relationships between the concentrations of the components and the extraction times were obtained by substituting M , N , L , α , β , and π into equation (4). The obtained quantitative transitivity expressions are listed in Table 4.

The kinetic behavior of drug concentration can be determined by applying the total statistic moment to the extraction kinetics, as summarized in Table 5. In addition, we obtained the similarity result of the total statistic moment, as listed in Table 6.

The maximum similarity between AST-IV and the additive component was 0.8984; thus, AST-IV is likely the main component controlling the extraction rate. However, the

content of the composition should also be considered, where the product of the two is the standard of evaluation. According to the information in Table 7, AST-IV is the main component controlling the extraction rate.

Table 3. Extraction kinetic parameters of total glycosides and the five main components.

Parameter	Total Glycosides	AST-IV	PF	LT	FA	LS	Additive Component
K/min^{-1}	16.05×10^{-6}	1.466×10^{-6}	11.82×10^{-6}	0.05339×10^{-6}	1.457×10^{-6}	3.082×10^{-6}	1.963×10^{-6}
$k1'/\text{min}^{-1}$	0.2235	0.6291	0.1730	0.2830	0.2384	0.1264	0.2487
$k2'/\text{min}^{-1}$	130.8	94.31	2.372	1.745	3.805	1.105	111.8
ρ_1	7.051	2.563	2.607	2.573	2.576	2.597	3.245
ρ_2	0.3210	1.069	1.046	1.154	0.453	0.787	0.674
$t_{\text{max}}/\text{min}$	94.94	300	47.99	781.0	719.0	719.9	720.0
$c_{\text{max}}/\%$	57.38	54.10	47.20	29.00	29.66	41.80	46.00
AUC/min	6.226×10^4	6.819×10^4	8.457×10^4	1.872×10^7	6.860×10^5	3.243×10^5	5.0923×10^5
$w_0/\%$	75.30	1.231	0.2560	0.3521	0.2100	0.467	2.516
P/%	5738	5410	4720	2900	2966	4180	4600
D/%	0.08480	0.02000	0.1194	0.0005550	0.03068	0.08098	0.06055

Table 4. Relationships between concentration (C) and extraction time (t) for the five main components.

	Relational Expression
AST-IV	$C = 0.1187e^{-0.00959t} - 0.2298e^{-0.0225t} + 0.02190e^{-0.0088t}$
PF	$C = 0.7269e^{-0.00201t} - 0.6963e^{-0.0625t} + 0.04799e^{-0.07597t}$
LT	$C = 0.2902e^{-0.00103t} - 0.1903e^{-0.0284t} + 0.07816e^{-0.01154t}$
FA	$C = 0.3063e^{-0.00305t} - 0.1887e^{-0.01768t} + 0.01432e^{-0.04416t}$
LS	$C = 0.4654e^{-0.00902t} - 0.4101e^{-0.00707t} + 0.1446e^{-0.0141t}$

Table 5. Total statistical moment parameters of various compounds in the BYHWD.

Parameter	Total Glycosides	AST-IV	PF	LT	FA	LS	Additive Component
MRT/min	96.73	86.22	14.68	64.53	22.43	72.10	104.69
VRT/min ²	86.22	96.2	7.584	41.60	50.20	80.02	108.07

Table 6. Similarity parameters of total statistic moment in the BYHWD.

	Total Glycosides	AST-IV	PF	LT	FA	LS	Additive Component
Total glycosides (effective components)	1	0.1098	0.7685	0.002792	0.0632	0.1823	0.1284
AST-IV	0.1098	1	0.1539	0.03097	0.6588	0.6828	0.8984
PF	0.7685	0.1539	1	0.003900	0.0883	0.2563	0.1802
LT	0.002792	0.03097	0.003900	1	0.05375	0.01856	0.02645
FA	0.06329	0.6580	0.0883	0.05375	1	0.4136	0.5742
LS	0.1823	0.6828	0.2563	0.01856	0.4136	1	0.7760
Additive component	0.1284	0.8984	0.1802	0.02640	0.5742	0.7760	1

Table 7. Product of similarity parameters and content of the BYHWD.

	Total Glycosides	AST-IV	PF	LT	FA	LS	Additive Component
Similarity of additive data	1	0.1098	0.7685	0.002792	0.0632	0.1823	0.1284
Similarity \times content	2.960	82.15	4.491	0.5564	7.368	20.80	184.8

3.7. Action Coefficients of the Kinetic Network

According to the previously discussed HPLC fingerprints of the BYHWD, we obtained the peak area values of 13 components, and the results are summarized in Table 8.

Table 8. Peak area values at different times for 13 components of the original herbal mixture.

Average Retention Time (min)	5 Min	10 Min	20 Min	30 Min	60 Min	90 Min	120 Min	180 Min	240 Min	360 Min	720 Min	1355 Min	1440 Min
3.39	477,789	503,330	686,965	524,721	572,198	644,160	577,595	611,243	619,056	653,347	655,351	1,054,145	1,206,922
5.72	1,714,996	1,832,252	2,077,599	1,896,874	2,331,715	2,573,756	2,261,854	2,385,237	2,814,849	2,643,691	2,349,501	3,444,613	3,864,146
7.49	150,639	572,886	702,495	620,750	549,683	679,000	584,515	749,073	608,900	804,443	860,854	1,673,152	937,343
10.35	823,603	91,477	1,147,259	124,004	68,864	250,291	1,111,596	126,141	1,192,171	135,977	1,257,381	1,925,657	1,872,837
13.23	883,314	1,081,969	1,510,304	1,629,265	125,011	537,224	3,146,488	4,585,570	4,553,217	4,948,196	5,502,817	7,333,328	8,083,948
22.65	1,280,253	1,070,115	1,602,922	1,493,914	2,595,508	1,791,472	1,876,407	2,389,710	2,016,905	2,574,613	2,122,311	3,650,321	3,919,484
38.55	285,418	312,803	395,585	366,656	1,066,898	393,072	379,575	326,211	356,300	325,626	301,266	475,478	449,841
40.26	129,901	500,075	238,799	155,218	228,087	1,632,093	222,357	152,379	1,291,733	696,912	479,320	407,426	165,495
48.02	749,934	822,291	1,187,851	1,142,140	1,375,508	1,992,421	1,875,622	179,447	1,203,844	292,330	99,423	135,279	967,129
52.12	500,843	612,545	746,073	831,971	2,187,140	1,860,377	1,630,272	2,597,072	1,797,012	2,896,386	2,403,598	142,326	2,142,757
57.3	176,380	445,776	148,598	167,340	397,890	455,110	213,213	75,222	126,402	162,541	139,202	181,702	130,122
61.49	253,481	276,938	241,488	318,408	606,205	613,445	359,062	400,048	481,896	128,604	449,955	115,779	61,445
63.57	151,775	145,948	280,280	362,128	501,849	805,806	741,438	867,384	934,550	116,489	95,788	1,008,009	59,506

Pajak software was used to effectively analyze large networks. We substituted the values in Table 8 into SPSS, and the resultant action coefficients are presented in Table 9.

Table 9. Action coefficients of 13 components of the original herbal mixture.

	1	2	3	4	5	6	7	8	9	10	11	12	13
1	1	−3.202	6.501	−1.981	−19.755	13.455	—	−21.328	38.527	50.059	−13.855	−19.374	−1.777
2	−0.287	1	1.914	—	−5.992	—	1.272	−12.262	—	44.878	−55.358	−55.677	−30.396
3	0.152	—	1	0.287	—	−2.402	−0.694	4.327	−5.850	−23.039	27.753	30.253	15.616
4	−0.019	−0.037	—	1	−0.107	−2.780	—	4.696	1.477	—	11.561	−7.057	—
5	−0.042	−0.143	0.280	−0.024	1	23.150	86.186	−1.701	−71.15	0.097	2.588	−8.084	−4.450
6	0.008	—	−0.057	−0.090	0.251	1	−0.016	1.703	—	—	—	0.949	1.038
7	0.199	—	−1.285	3.774	—	—	1	2.654	−8.322	−28.757	31.286	42.298	19.776
8	−0.076	−0.239	0.492	−0.309	−1.464	0.358	—	1	3.108	11.156	−12.657	−15.887	−7.650
9	0.024	0.075	−0.154	—	—	−0.030	−0.119	—	1	−3.447	4.314	5.057	2.422
10	—	0.020	−0.040	0.006	0.131	−0.152	−0.027	0.247	−0.227	1	1.349	—	0.651
11	−0.001	−0.005	0.009	0.009	—	0.043	16.47	−0.100	0.051	0.244	1	−0.220	−0.181
12	−0.005	−0.014	0.030	—	—	0.018	2.365	−0.044	0.190	0.671	−0.695	1	−0.469
13	−0.009	−0.030	0.058	−0.008	−0.181	0.178	0.040	−0.338	0.342	1.398	−2.151	−1.766	1

The action coefficient reflects the relationship between two components, where larger values indicate stronger effects on each other. A positive value indicates the promotion of dissolution, a negative value indicates the inhibition of dissolution, and '—' indicates no interaction. The action coefficient between a component and itself is 1.

3.8. Network Diagrams Visualized Using Pajek Software

The action coefficients in Table 9 were imported into Pajek software to obtain the network action diagrams of the 13 components shown in Figures 8 and 9.

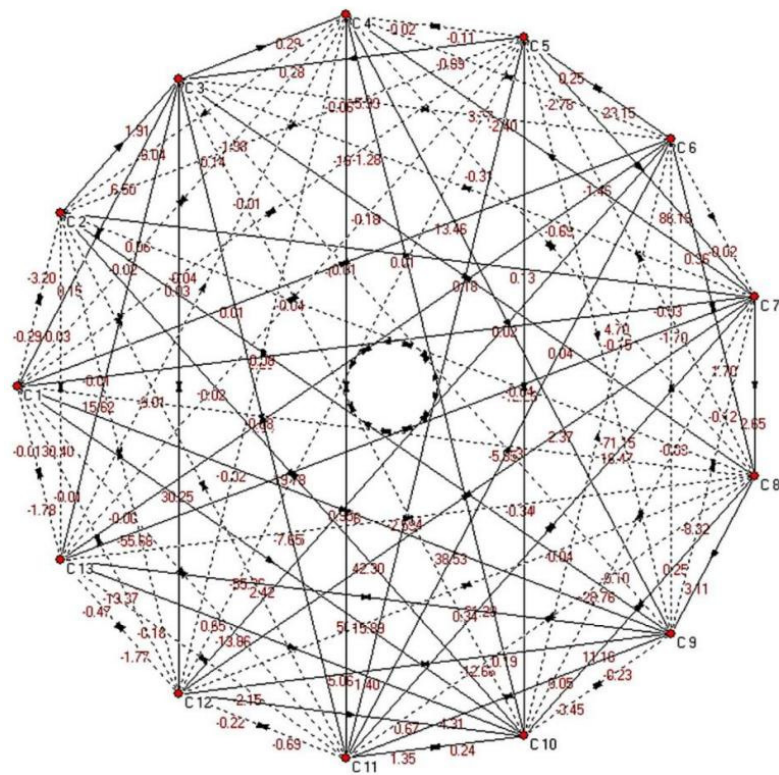


Figure 8. Plane network diagram of 13 components in the BYHWD.

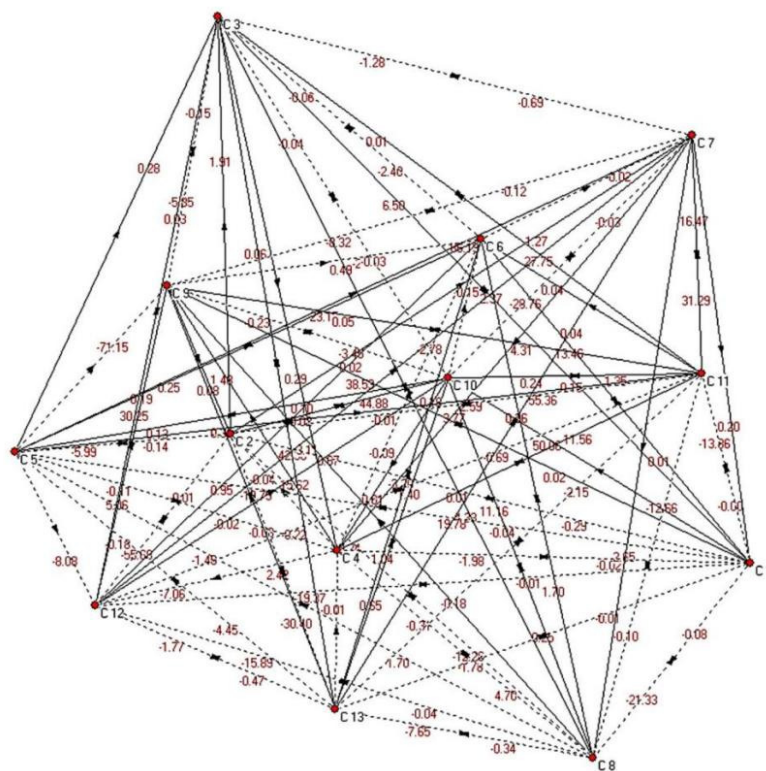


Figure 9. Stereoscopic network diagram of 13 components in the BYHWD.

Given the complex composition of TCMs, topological analysis can simplify the interaction network of the components in a very intuitive way [22]. The solid and dotted lines in Figures 8 and 9 correspond to the positive and negative numbers, respectively, in Table 9.

3.9. Network Topological Analysis of BYHWD Extraction Dynamics

Using the data in Table 3, the network action coefficients for the 13 fingerprint peaks were substituted into Pajek software [23] to obtain the results presented in Table 10. In this network, the network diameter was 0.287, the average degree was 21.84, and the network density was 83%.

Table 10. Characteristics for each node in the network.

	1	2	3	4	5	6	7	8	9	10	11	12	13
Out-degree	11	9	10	8	12	8	9	11	9	10	11	10	12
In-degree	11	9	11	9	7	10	9	11	10	10	11	11	11
Node degree	22	18	21	17	19	18	18	22	19	20	22	21	23
Clustering coefficient	0.81	0.85	0.82	0.85	0.84	0.85	0.84	0.81	0.84	0.83	0.81	0.82	0.81

4. Discussion

Some extraction process models of extraction kinetics have been reported [24], but they do not consider the cellular structure of the herbs [25]. In addition, herbs can absorb solvent and swell to several times their original size [26,27]. The tendency of certain components to decompose during the typical high-temperature extraction process used in TCMs has not been considered. In this work, a general model for the Laplace-transformed dissolution kinetics of TCMs was established to provide a theoretical foundation for quantitative research and the further optimization of the TCM extraction process [8].

The experimental extraction data for the total glycosides and the components AST-IV, PF, LT, FA, and LS were consistent with the predictions of the three-compartment model ($p < 0.01$). As $K \neq 0$, we have $k_1' \neq k_2'$, and $\rho_1, \rho_2 \neq 1$, indicating that the apparent concentrations in the different chambers were not equal. For all components, $\rho_1 \gg \rho_2$ and $k_2' \gg k_1'$, indicating that component diffusion was faster in the solution chamber than in the other two chambers [28]. In future studies, certain TCM ingredients, such as hard or irregularly shaped herbs, may require models that have more than three compartments [29]. Additionally, we studied a closed extraction system, and the modeling of open systems (e.g., the diacolation method) and insoluble components need further discussion. Nevertheless, the method and results presented here (Table 3) for the three-compartment model can be easily generalized into a multi-compartment linear model.

According to the information in Table 1, the measured concentrations of glycoside components in the solvent first increased during extraction and then decreased, owing to elimination at high temperatures. Therefore, the extraction time of the BYHWD should not be too long. We obtained the total statistic moment values for all components (Table 5). AST-IV was the most additive component, and it is likely the main component controlling the extraction rate (Table 6). In addition to similarity, the content of the composition should be considered, where the product of the two is regarded as the standard of evaluation. The component with the largest product value is the rate-limiting component [30–32]. Here, the results showed that the bioactive ingredient AST-IV was the main component controlling the extraction rate (Table 7).

In the obtained topological network for the BYHWD consisting of 13 ingredients as nodes, the network density, that is, the probability of a connection between two arbitrary nodes, was 83%, which indicated that the nodes in the network had quite close interactions. However, this is only a relative conclusion; if the network scale were increased, then the density value would reduce substantially, and it may be difficult to obtain valuable conclusions by comparing the network densities of different networks.

The use of the node degree can compensate for the inadequacy of network density: the former has no relationship with the network scale, whereas the latter does. For example, AST-IV had maximum and minimum out-degree values of 12 and 7, respectively, which indicated that AST-IV had a significant effect on the other 12 components in the extraction process but was less affected by the others. AST-IV promoted the dissolution of LS and LT and inhibited that of PF and FA. When discussing the network relationships among AST-IV, PF, LT, FA, and LS, it is possible to deduce whether a component promoted or inhibited the dissolution according to the sign of the action coefficient.

The average degree also shows that the nodes are densely linked, although some have no effect on each other. These unlinked nodes reduce the average node degree for the entire network, which conforms to the normal state of TCM compounds. Therefore, the average node degree determined here (21.84) demonstrates that this network system had a high degree of condensation. The nodes in the extraction network of the BYHWD were closely connected.

Nevertheless, in the current study, the node degree was calculated by assuming an unweighted scale-free network [33]. Weighting of the nodes may be necessary to further explain the mutual promotion and inhibition among the 13 ingredients in the BYHWD.

5. Conclusions

In summary, research on the extraction technology used for Chinese medicinal materials is an important link in the modernization of Chinese medicinal preparations. In this article, a set of algebraic calculus equations was established to obtain the kinetic parameters of each bioactive ingredient in the BYHWD. After determining these functional expressions, the obtained kinetic parameters were analyzed to locate the main rate-control components. The kinetic network was further represented by a network topology diagram for the various components in the BYHWD, and the dissolution kinetics and dissolution relationships of the five principal components were discussed in this context. These theoretical and experimental results could be used to quantitatively simulate and optimize TCM and food extraction processes.

Author Contributions: Conceptualization: F.H.; data curation: Y.T.; formal analysis: Y.T.; funding acquisition: F.H.; investigation: Y.Z. (Yiqun Zhou); methodology: Y.Z. (Yutian Zhang); project administration: W.L.; resources: W.L.; software: Z.L.; supervision: Z.L.; validation: K.D.; visualization: K.D.; writing—original draft: Y.T.; writing—review and editing: Y.T. All authors have read and agreed to the published version of the manuscript.

Funding: This work was supported by the National Natural Science Foundation of China (grant Nos. 81874344 and 81874507), the Hunan Provincial Department of Education's Outstanding Youth Project in Scientific Research (grant No. 21B0382), the Natural Science Foundation of Hunan Province (grant Nos. 2021JJ80058 and 2021JJ30514), the Project of Hunan Administration of Traditional Chinese Medicine (grant Nos. 2021073 and 2021204), the Pharmaceutical Open Fund of Domestic First-Class Disciplines (Cultivation) of Hunan Province (grant Nos. 2021YX04 and 2018YX11), and the University-Level Scientific Research Fund of Hunan University of Chinese Medicine (grant No. 2020XJJ029). The funders had no role in the study design; in the collection, analysis, or interpretation of data; in the writing of the report; or in the decision to submit the article for publication.

Institutional Review Board Statement: Not applicable.

Informed Consent Statement: Not applicable.

Data Availability Statement: The datasets used and/or analyzed during the current study are available from the corresponding author on reasonable request.

Conflicts of Interest: The authors declare no conflict of interest.

Abbreviations

TCM	Traditional Chinese Medicine
BYHWD	buyang huanwu decoction
AST-IV	Astragaloside IV
PF	paeoniflorin
LT	Laetrile
FA	ferulic acid
LS	ligustrazine
AUC	area under the curve
MIC	compartment in cell
CIS	compartment in solution
CMCP	Chinese medicine compound prescription

References

- Zhou, J.; Deng, K.W.; Duan, X.P.; He, F.Y. Study on calculation of fingerprint total quantum statistical moment(TQSM) and to decide integral condition. *Chin. Arch. Tradit. Chin. Med.* **2012**, *30*, 505–508.
- He, F.Y.; Deng, K.W.; Luo, J.Y.; Liu, W.; Liu, W.L.; Deng, C.Q. Fundamentally study on mathematical kinetic model of component extraction from FTCM. *China J. Chin. Mater. Medica* **2007**, *32*, 490–495.
- Jadhav, D.; Rekha, B.N.; Gogate, P.R.; Rathod, V.K. Extraction of vanillin from vanilla pods: A comparison study of conventional soxhlet and ultrasound assisted extraction. *J. Food Eng.* **2009**, *93*, 421–426. [[CrossRef](#)]
- Suganya, T.; Renganathan, S. Optimization and kinetic studies on algal oil extraction from marine macroalgae *Ulva lactuca*. *Bioresour. Technol.* **2011**, *107*, 319–326. [[CrossRef](#)] [[PubMed](#)]
- Shang, E.; Su, S.; Zeng, H.; Zhu, Z.; Duan, J. A novel modeling method to evaluate the bioactive contributions of compositions in traditional Chinese medicine. *Chemom. Intell. Lab. Syst.* **2016**, *159*, 151–154. [[CrossRef](#)]
- Aguilera, J.M.; Escobar, G.A.; Delvalle, J.M.; Martin, R. Ethanol extraction of red peppers: Kinetic studies and microstructure. *Int. J. Food Sci. Technol.* **1987**, *22*, 225–232. [[CrossRef](#)]
- Vetal, M.D.; Lade, V.; Rathod, V.K. Extraction of ursolic acid from *Ocimum sanctum* leaves: Kinetics and modeling. *Food Bioprod. Process.* **2012**, *90*, 793–798. [[CrossRef](#)]
- Leal, P.F.; Almeida, T.S.; Prado, G.; Prado, J.M.; Meireles, M.A.A. Extraction kinetics and anethole content of fennel (*Foeniculum vulgare*) and anise seed (*Pimpinella anisum*) extracts obtained by Soxhlet, ultrasound, percolation, centrifugation, and steam distillation. *Sep. Sci. Technol.* **2011**, *46*, 1848–1856. [[CrossRef](#)]
- Haghshenas, H.; Sadeghi, M.T.; Ghadiri, M. Mathematical modeling of aroma compound recovery from natural sources using hollow fiber membrane contactors with small packing fraction. *Chem. Eng. Process. Process Intensif.* **2016**, *102*, 194–201. [[CrossRef](#)]
- Fick, A. On liquid diffusion. *Membr. Sci.* **1995**, *100*, 33–38. [[CrossRef](#)]
- Nagy, J.; Veress, T. Systematic error for extraction of controlled substances from plant/fungal materials. *J. Chromatogr. Sci.* **2020**, *58*, 985–991. [[CrossRef](#)]
- Yuan, H.F.; Luo, J.Y.; Deng, K.W.; Liu, X.J.; Yang, Y. A survey on status and research method of pharmacokinetics of formula Chinese materia medica. *Chin. Tradit. Herb. Drugs* **2005**, *36*, 1583.
- Lewicki, P.P. Effect of pre-drying treatment, drying and rehydration on plant tissue properties: A review. *Int. J. Food Prop.* **1998**, *1*, 1–22. [[CrossRef](#)]
- Zhang, Y.-T.; Liu, W.-L.; Tang, Y.; Yang, Y.-T.; Xiao, M.-F.; Zhou, Y.-Q.; Zhou, J.; He, F.-Y. A novel kinetic model for dissolution of herbal medicine. *Dissolut. Technol.* **2018**, *25*, 28–38. [[CrossRef](#)]
- Adnadjevic, B.; Koturevic, B.; Jovanovic, J. Isothermal kinetics of ethanolic extraction of total hypericin from pre-extracted *Hypericum perforatum* flowers. *Phytochem. Anal.* **2021**, *32*, 757–766. [[CrossRef](#)] [[PubMed](#)]
- Zou, J.B.; Zhang, X.F.; Tai, J.; Wang, J.; Cheng, J.X.; Zhao, C.B.; Feng, Y.; Wang, Y.; Liang, Y.L.; Shi, Y.J. Extraction kinetics of volatile oil from galangal by steam distillation. *China J. Chin. Mater. Medica* **2018**, *43*, 4231–4239. [[CrossRef](#)]
- He, F.-Y.; Deng, K.-W.; Liu, W.-L.; Shi, J.-L.; Wu, Y.; Liu, W.; He, Q.-P.; Li, B. Experimental studies on pharmacokinetics of three components in Buyanghuanwu injection on base of total quantum statistical moment. *China J. Chin. Mater. Medica* **2013**, *38*, 253–262.
- Horkovics-Kovats, S. Disintegration rate and properties of active pharmaceutical ingredient particles as determined from the dissolution time profile of a pharmaceutical formulation: An inverse problem. *J. Pharm. Sci.* **2014**, *103*, 456–464. [[CrossRef](#)]
- Tang, Y. Establishment of quantitative determination methods of total glycoside groups composition in Chinese materia medica by differential anthrone-sugar hydrazone. *Chin. Tradit. Herb. Drugs* **2014**, *45*, 2333–2338.
- Chinese Pharmacopoeia Commission. *Pharmacopoeia of the People's Republic of China*; China Medical Science Press: Beijing, China, 2020; Volume 20.
- Dai, Y.; Wang, D.; Zhao, M.; Yan, L.; Zhu, C.; Li, P.; Qin, X.; Verpoorte, R.; Chen, S. Quality markers for *Astragali radix* and its products based on process analysis. *Front. Pharmacol.* **2020**, *11*, 554777. [[CrossRef](#)]

22. Capparucci, C.; Gironi, F.; Piemonte, V. Equilibrium and extraction kinetics of tannins from chestnut tree wood in water solutions. *Asia Pac. J. Chem. Eng.* **2011**, *6*, 606–612. [[CrossRef](#)]
23. Zhu, D.Z.; Jun, W.U.; Tan, Y.J.; Deng, H.Z. Construction of complex networks based on degree distribution. *Comput. Simul.* **2007**, *24*, 130–136.
24. Aoyama, T.; Omori, T.; Watabe, S.; Shioya, A.; Ueno, T.; Fukuda, N.; Matsumoto, Y. Pharmacokinetic/pharmacodynamic modeling and simulation of rosuvastatin using an extension of the indirect response model by incorporating a circadian rhythm. *Biol. Pharm. Bull.* **2010**, *33*, 1082–1087. [[CrossRef](#)]
25. Wu, Q.; Li, M.-Y.; Li, H.-Q.; Deng, C.-H.; Li, L.; Zhou, T.-Y.; Lu, W. Pharmacokinetic-pharmacodynamic modeling of the anticancer effect of erlotinib in a human non-small cell lung cancer xenograft mouse model. *Acta Pharmacol. Sin.* **2013**, *34*, 1427–1436. [[CrossRef](#)] [[PubMed](#)]
26. Deng, J.L.; Deng, K.W.; Liu, W.L.; Shi, J.L.; Yang, Y.T.; Luo, J.Y.; He, F.Y. Validation of chromatogram pharmacokinetic model, a pharmacokinetics for multiple components in Chinese materia medica with fingerprint chromatography. *China J. Tradit. Chin. Med. Pharm.* **2013**, *28*, 3367–3373.
27. He, F.Y.; Deng, K.W.; Liu, W.L.; Shi, J.L.; Zou, H.; Tang, Y.; Liu, P.A.; Zhou, H.H. Reactive essence between Chinese materia medica formula and human body: Multiple genetic chromatodynamokinetics with ‘co-network compatibility and rainbow potential’. *Chin. J. Exp. Tradit. Med. Formulae* **2011**, *17*, 240–247.
28. He, F.; Deng, K.; Zou, H.; Qiu, Y.; Chen, F.; Zhou, H. Study on differences between pharmacokinetics and chromatopharmacodynamics for Chinese materia medica formulae. *China J. Chin. Mater. Medica* **2011**, *36*, 136–141.
29. Chen, F.; He, X.; Fang, B.; Wang, S. Simultaneous quantitative analysis of six proton-pump inhibitors with a single marker and evaluation of stability of investigated drugs in polypropylene syringes for continuous infusion use. *Drug Des. Dev. Ther.* **2020**, *14*, 5689–5698. [[CrossRef](#)] [[PubMed](#)]
30. Muhammad, A.; Younas, M.; Rezakazemi, M. Quasi-dynamic modeling of dispersion-free extraction of aroma compounds using hollow fiber membrane contactor. *Chem. Eng. Res. Des.* **2017**, *127*, 52–61. [[CrossRef](#)]
31. Gul, R.; Jan, S.U.; Faridullah, S.; Sherani, S.; Jahan, N. Preliminary phytochemical screening, quantitative analysis of alkaloids, and antioxidant activity of crude plant extracts from *Ephedra intermedia* indigenous to Balochistan. *Sci. World J.* **2017**, *2017*, 5873648. [[CrossRef](#)] [[PubMed](#)]
32. Miao, W.G.; Tang, C.; Ye, Y.; Quinn, R.J.; Feng, Y. Traditional Chinese medicine extraction method by ethanol delivers drug-like molecules. *Chin. J. Nat. Med.* **2019**, *17*, 713–720. [[CrossRef](#)]
33. Gul, R.; Jan, S.U.; Ahmad, M.; Faridullah, S.; Akhtar, M. Formulations, characterization, in vitro and ex vivo release of *Ephedra* extract from topical preparations using dialysis cellulose membrane and natural rabbit skin. *Dissolut. Technol.* **2017**, *24*, 24–30. [[CrossRef](#)]